Proximity induced interface bound states in superconductor-graphene junctions

P. Burset[1], W. Herrera[2] and A. Levy Yeyati[1]
[1] *Departamento de Física Teórica de la Materia Condensada C-V, Facultad de Ciencias, Universidad Autónoma de Madrid, E-28049 Madrid, Spain*
[2] *Departamento de Física, Universidad Nacional de Colombia, Bogotá, Colombia*

(Dated: December 4, 2018)

We show that interface bound states are formed at isolated graphene-superconductor junctions. These states arise due to the interplay of virtual Andreev and normal reflections taking place at these interfaces. Simple analytical expressions for their dispersion are obtained considering interfaces formed along armchair or zig-zag edges. It is shown that the states are sensitive to a supercurrent flowing on the superconducting electrode. The states provide long range superconducting correlations on the graphene layer which may be exploited for the detection of crossed Andreev processes.

PACS numbers: 73.23.-b, 74.45.+c, 74.78.Na, 73.20.-r

Introduction: Several striking transport properties have been predicted to emerge from the peculiar electronic band structure of single atom graphite layers, known as graphene [1]. Of particular interest is the case of a graphene layer in contact with a superconducting electrode, a situation which has been explored in several recent experiments [2]. Here, as in the case of normal metals, the mechanism which dominates the electronic transport at subgap energies is the Andreev reflection, i.e. the conversion of incident electrons into reflected holes with the creation of Cooper pairs in the superconductor. However, while in the case of normal metals the reflected hole has typically the opposite mean velocity to the incident electron (*retroreflection*) in the case of graphene it is possible to have Andreev reflections with a *specular* character, as first shown in [3].

Transport and electronic properties at graphene-superconductor junctions have been analyzed in several works [4]. It has been shown that the special character of Andreev reflection in graphene leads to modifications in the differential conductance compared to that of conventional N-S junctions [3, 5]. The effect on the local density of states (LDOS) has been studied in Refs. [6, 7]. The properties of bound states arising from multiple Andreev reflections in S-graphene-S junctions have been analyzed in Refs. [8]. However, as we show in this work, the special electronic properties of graphene are such that bound states can be formed even at *isolated* single junctions.

The mechanism for the emergence of these states can be understood from the scheme depicted in the left panel of Fig. 1. As is usually assumed the junction can be modeled as an abrupt discontinuity between two regions described by the Bogoliubov-de Gennes-Dirac equation, taking a finite superconducting order parameter Δ and large doping $E_F^S \gg \Delta$ on the superconducting side and zero order parameter and small doping $E_F \sim \Delta$ on the *normal* side. For the analysis it is instructive to include an artificial intermediate normal region with $\Delta = 0$ and $E_F^I = E_F^S$, whose width, d, can be taken to zero at the end of the calculation. This intermediate region allows

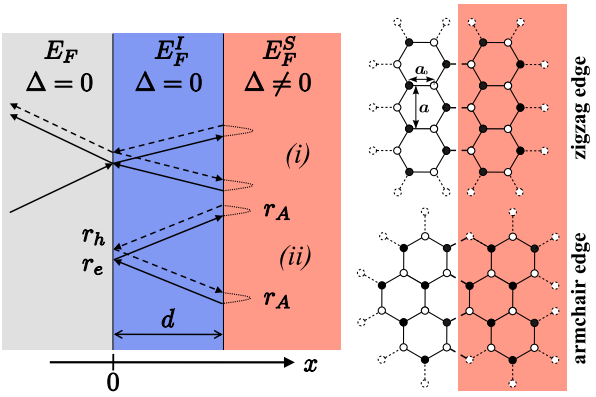

FIG. 1: (Color online) Simple model for the emergence of IBSs (left panel). It illustrates the scattering processes taking place at a graphene-superconductor interface with an intermediate heavily doped normal graphene region of width d. Cases (i) and (ii) correspond to the case $\hbar vq < |E \pm E_F|$ and $\hbar vq > |E \pm E_F|$ respectively with $\Delta > E > E_F$. (Right panel) Graphene-superconductor junctions along different edges. On the superconducting side (shaded areas) the on-site order parameter Δ is finite and the doping level is high ($E_F^S \gg \Delta$).

to spatially separate normal reflection due to the Fermi energy mismatch from the Andreev reflection associated to the jump in Δ. As shown in Fig. 1 (case i), an incident electron from the normal side with energy E and parallel momentum $\hbar q$ such that $\hbar vq < |E - E_F|$ is partially transmitted into the intermediate region and after a sequence of normal and Andreev reflections would be reflected as a hole. This process can either correspond to retro or specular Andreev reflection depending on whether $E < E_F$ or $E > E_F$ [3]. For $\hbar vq \geq |E \pm E_F|$ neither electron or holes can propagate within the graphene normal region. However, virtual processes like the one depicted in Fig. 1 (case ii) would be present. These correspond to sequences of Andreev and normal reflections within the intermediate region. A bound state emerges when the total phase ϕ accumulated in such processes reach the resonance condition $\phi = 2n\pi$.

The aim of the present work is to demonstrate the existence of these interface bound states (IBS) and to analyze their properties for different types of graphene-superconductor junctions. After completing the analysis for the case of the simple model sketched above, which implicitly assumes a decoupling of the two valleys in the graphene band structure, we consider more microscopic models for junctions formed along armchair or zig-zag edges. We study the effect of an additional potential barrier at the interface and the possibility to modify the states by a supercurrent flowing through the superconductor. We finally discuss the potential use of these states for the generation of non-locally entangled Andreev pairs.

It is quite straightforward to determine the dispersion relation for the IBS from the model represented in the left panel of Fig. 1. The phase accumulated by a sequence of normal and Andreev reflections in the intermediate region can be obtained from the corresponding coefficients r_e, r_h and r_A. Following Ref. [3] one obtains

$$r_{e,h} = e^{i\alpha^I_{e,h}} \frac{e^{-i\alpha^I_{e,h}} - e^{-i\alpha_{e,h}}}{e^{i\alpha^I_{e,h}} + e^{-i\alpha_{e,h}}}, \qquad (1)$$

where $\alpha^{(I)}_{e,h} = \arcsin \hbar v q/(E \pm E^{(I)}_F)$. The condition $E^I_F \gg \Delta, E, \hbar v q$ allows to take $\alpha^I_{e,h} \simeq 0$. On the other hand, in the region of evanescent electron and hole states for graphene ($|\hbar v q| > |E \pm E_F|$) $r_{e,h}$ become a pure phase factor $e^{i\varphi_{e,h}}$, with $\varphi_{e,h} = -2\mathrm{sign}(q/(E \pm E_F)) \arctan e^{\lambda_{e,h}}$ and $\lambda_{e,h} = \mathrm{sign}(q)\mathrm{arcosh}(\hbar v q/|E \pm E_F|)$. For the Andreev reflection coefficient between regions I and S one has $r_A = e^{i\varphi_A}$ where $\varphi_A = \arccos E/\Delta$, as it corresponds to the Andreev reflection at an ideal N-S interface with $E^S_F \gg \Delta$ [9]. In the limit $d \to 0$ the total phase accumulated is thus $\phi = 2\varphi_A + \varphi_e + \varphi_h$, from which one obtains the following dispersion relation

$$\frac{E}{\Delta} = \pm \frac{e^{(\lambda_e+\lambda_h)/2} - \mathrm{sign}(E^2 - E_F^2) e^{-(\lambda_e+\lambda_h)/2}}{2\sqrt{\cosh\lambda_e \cosh\lambda_h}}. \qquad (2)$$

This dispersion simplifies to $E/\Delta = \pm \hbar v q/\sqrt{(\hbar v q)^2 + \Delta^2}$ at the charge neutrality point (i.e. for $E_F = 0$). In this case the IBS approaches zero energy for $q \to 0$ and tend asymptotically to the superconducting gap for large q. Notice also that the decay of the states into the graphene bulk region ($x < 0$ in the left panel of Fig. 1) is set by $e^{x/\xi_{e,h}}$, where $\xi_{e,h} = \hbar v/(|E \pm E_F| \sinh(\lambda_{e,h}))$ for the electron and hole components respectively, which can be clearly much larger than the superconducting coherence length $\xi_0 = \hbar v/\Delta$ when $E_F \ll \Delta$. It is also interesting to notice that the IBSs survive when $E_F > \Delta$, i.e. in the regime corresponding to the usual Andreev retroreflection, but with a much smaller spatial extension.

In order to analyze the existence and the characteristics of the IBSs for different types of graphene-superconductor junctions we make use of the Green function formalism based on tight-binding models for these junctions which was introduced in Ref. [7]. Within this formalism the retarded green functions at the interface $\check{\hat{G}}(E,q)$ are given by $\left[\check{\hat{g}}^{-1} - \check{\hat{\Sigma}}\right]^{-1}$, where $\check{\hat{g}}$ corresponds to the surface of the uncoupled semi-infinite graphene layer and $\check{\hat{\Sigma}}$ is the self-energy associated to the coupling with the superconductor. In general all these quantities have a 2×2 structure both in the sublattice (indicated by the hat symbol) and the Nambu (indicated by the check symbol) spaces. Once these quantities for each type of interface have been determined, the existence of an IBS can be established by analyzing the equation $\det\left[\check{\hat{g}}^{-1} - \check{\hat{\Sigma}}\right] = 0$.

Interface along an armchair edge: We first consider an interface constructed along an armchair edge, as schematically depicted in the right panel of Fig. 1. In a rather generic way one can write $\check{\hat{g}} = \hat{g}_e(\check{\tau}_0 + \check{\tau}_z)/2 + \hat{g}_h(\check{\tau}_0 - \check{\tau}_z)/2$ and $\check{\hat{\Sigma}}/t_g = \beta\check{\tau}_z\check{g}_{BCS}\check{\tau}_z + \gamma\check{\tau}_z\hat{\sigma}_x$, where $\hat{g}_{e,h}$ describe the propagation of e and h components in the uncoupled graphene layer, $\check{g}_{BCS} = g\check{\tau}_0 + f\check{\tau}_x$ with $g = -Ef/\Delta = -E/\sqrt{\Delta^2 - E^2}$ being the BCS dimensionless Green functions, and β and γ are parameters which allow to control the transparency and the type of interface. As discussed in Ref. [7] $\gamma = 0$ corresponds to a model in which the coherence between the sublattices of graphene is broken on the superconducting side (bulk-BCS model), whereas for $\beta = \sqrt{3}/2$ and $\gamma = 1/2$ corresponds to the ideal case where superconductivity is induced on the graphene layer by a superconducting electrode deposited on top, thus leading to a heavily doped graphene superconductor (HDSC).

To make further analytical progress we take the limit $E, \Delta, \hbar v q \ll t_g$ in $\hat{g}_{e,h}$ of Ref. [7], where t_g denotes the hopping element between neighboring sites in the graphene layer. In this case and for $\hbar v q > |E \pm E_F|$, $\hat{g}_{e,h}$ adopt the form $t_g\hat{g}_{e,h} = -\frac{1}{2}\left[\sqrt{3}\left(\mu_{e,h}\hat{\sigma}_0 + \nu_{e,h}\hat{\sigma}_y\right) \pm \hat{\sigma}_x\right]$, where $\mu_{e,h} = \mathrm{sign}(q)/\sinh\lambda_{e,h}$ and $\nu_{e,h} = \mathrm{sign}(E \pm E_F)/\tanh\lambda_{e,h}$. The Green functions matrix has the property $\hat{g}^{-1}_{e,h} = -t_g^2\hat{g}^T_{e,h} \mp t_g\sigma_x$. Using this property and the definition for the self-energy the equation for the IBSs in this case becomes

$$\det\left[t_g^2\hat{g}_h\hat{g}_e + \beta g t_g\left(\hat{g}_e + \hat{g}_h\right) + \gamma t_g\left(\hat{\sigma}_x\hat{g}_e - \hat{g}_h\hat{\sigma}_x\right) - (\beta^2 + \gamma^2)\right] = 0. \qquad (3)$$

For the HDSC model (i.e. $\beta = \sqrt{3}/2$ and $\gamma = 1/2$) the equation for the IBSs reduce to the one already found within the simple analytical model (Eq. (2)). This leads to a single root for arbitrary doping which is four-fold degenerate due to valley and spin symmetry. Fig. 2 shows a color-scale plot of the spectral density at a distance

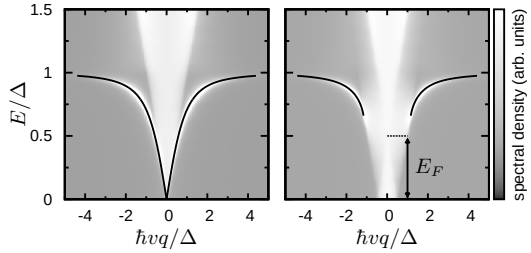

FIG. 2: Gray-scale plot of the spectral density at a distance $\sim \xi_0$ from the interface defined along an armchair edge. The results were obtained using the HDSC model of Ref. [7] for $E_F = 0$ (left panel) and $E_F = \Delta/2$ (right panel). The full lines indicate the position of the IBS determined from Eq. (2).

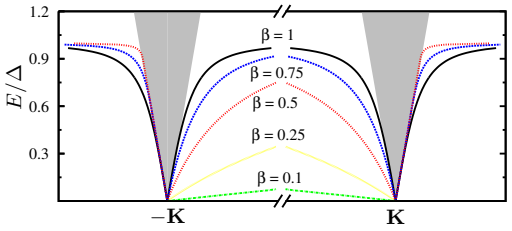

FIG. 3: (Color online) Dispersion relation for the IBSs on a zig-zag interface for decreasing parameter β controlling the coupling with the superconductor. The parallel momentum q in Eq. (6) is measured from the Dirac points at $K = \pm 2\pi/3a$.

$\sim \xi_0$ from the interface on the graphene layer with two different doping conditions. The full lines correspond to the IBS dispersion obtained by solving Eq. (2). As can be observed, the minimal energy for the IBSs, E_{min}, depends on E_F. Further analysis of Eq. (2) reveals that it satisfies the cubic equation $E_{min}^3 + E_{min}^2 E_F - \Delta^2 E_F = 0$, thus evolving between 0 and Δ as E_F increases. The transition between $E_{min} > E_F$ and $E_{min} < E_F$ occurs at $E_F = \Delta/\sqrt{2}$. The presence of the IBSs manifests also in the appearance of singularities in the LDOS around $E = \pm\Delta$ (see Ref. [7]). The behavior of the LDOS is analyzed in more detail below.

On the other hand, for the bulk-BCS model (i.e. $\gamma = 0$ and $\beta \in (0, 1)$) one obtains

$$\frac{3}{2}\beta^2 g^2(\mu_e\mu_h + \nu_e\nu_h - 1) + \sqrt{3}\beta g(\mu_e + \mu_h)(1+\beta^2) + \frac{\beta^2(1+2\beta^2)}{2} + \frac{3}{4}(1+2\beta^2)(\nu_e\nu_h - \mu_e\mu_h) + \frac{1}{4} = 0. \quad (4)$$

In this case the degeneracy associated to the two valleys in the band-structure of graphene is generally broken (except for $E_F = 0$). The roots gradually evolve towards the linear dispersion $|E + E_F| = \hbar v q$ as $\beta \to 0$, which corresponds to the armchair edge state of the isolated graphene layer [10].

Interface along a zig-zag edge: We now consider an interface along a zig-zag edge as illustrated in the right panel of Fig. 1. The Green functions for the semi-infinite zig-zag edge can be obtained following the same formalism as in Ref. [7]. In the continuous limit $\hat{g}_{e,h}$ becomes

$$t_g \hat{g}_{e,h} = \begin{pmatrix} ie^{-i\alpha_{e,h}} & \mp e^{i\pi/3} \\ \mp e^{-i\pi/3} & 0 \end{pmatrix}, \quad (5)$$

where as in Eq. (1) $\sin\alpha_{e,h} = (\hbar v q)/(E \pm E_F)$ but with q measured with respect to the point $\mathbf{K} = 2\pi/3a$, where a is the lattice constant indicated in the right panel of Fig. 1. There exists an additional branch where q is measured from the opposite Dirac point at $-\mathbf{K}$. The self-energy due to the coupling with the superconductor is in this case $\check{\tilde{\Sigma}} = \beta t_g(\hat{\sigma}_0 + \hat{\sigma}_z)\left(\check{\tau}_z \check{g}_{BCS} \check{\tau}_z\right)/2$. The equation for the IBSs then becomes

$$\frac{E}{\Delta} = \pm \frac{e^{(\lambda_e+\lambda_h)/2} - \mathrm{sign}(E^2 - E_F^2)\beta^2 e^{-(\lambda_e+\lambda_h)/2}}{\sqrt{(e^{\lambda_e} + \beta^2 e^{-\lambda_e})(e^{\lambda_h} + \beta^2 e^{-\lambda_h})}}, \quad (6)$$

which looks very similar to Eq.(2) except for the presence of the parameter β controlling the coupling and the already mentioned redefinition of the parallel momentum q. An interesting property of zig-zag edges is the presence of zero energy states for total parallel momentum between $(-\mathbf{K}, \mathbf{K})$ and $E_F = 0$ [11]. When the coupling to the superconductor is turned on by increasing the parameter β, one observes that the zero energy states evolve acquiring a finite slope. These states can thus be identified with the IBS for this type of interface. This is illustrated in Fig. 3. When the coupling parameter β reaches 1 the usual dispersion of the simplest analytical model is recovered.

Effect of a supercurrent: a supercurrent flowing on the superconducting side of the junction modifies the spatial variation of the phase of the order parameter which produces a Doppler shift in the energy of the quasiparticles. This shift, obtained from the Bogoliubov-de Gennes-Dirac equations within the Andreev approximation, is given by $\eta = (\hbar v)^2 q_s q / E_F^S$, where $\hbar q_s$ is the momentum of the Cooper pairs assumed to be parallel to the interface. This result is equivalent to the one found in Refs. [12] for conventional and two-band superconductors. Notice that for this analysis we go beyond the limit $E_F^S \to \infty$ taken in the initial simple model. The expression for the reflection coefficients of Eq. (1) still holds but $\alpha_e^I \simeq -\alpha_h^I \equiv \alpha^I = \arcsin \hbar v q / E_F^S$ is kept finite. On the other hand, the phase of the Andreev reflection coefficient between the intermediate region and the current-carrying superconductor becomes $\varphi_A = \arccos E'/\Delta(q_s)$, where $E' = E + \eta$. At zero temperature, due to Landau criterion, the order parameter is unaffected by the supercurrent while $\hbar v q_s \lesssim \Delta(0)$ [12]. Therefore, in this condition, $\Delta(q_s) \simeq \Delta(0) \equiv \Delta$. For the case $E > E_F$ we thus get the following modified equation for the IBSs

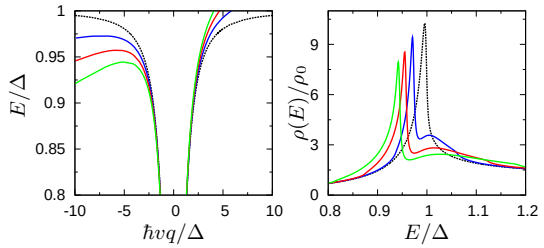

FIG. 4: (Color online) Effect of a supercurrent flowing on the superconducting electrode on the dispersion relation (left panel) and on the local density of states at a distance $\sim \xi_0/10$ from the interface normalized to $\rho_0 = \Delta(a/\hbar v)^2/2\pi$ (right panel). The results correspond to $\hbar v q_s/\Delta = 0.0, 0.25, 0.5$ and 0.75 with $E_F^S = 100\Delta$.

within the simple model sketched in Fig. 1

$$\frac{E'}{\Delta} = \pm \frac{\sinh(\lambda_e + \lambda_h)/2 + \sin\alpha^I \sinh(\lambda_e - \lambda_h)/2}{\sqrt{(\cosh\lambda_e - \sin\alpha^I)(\cosh\lambda_h + \sin\alpha^I)}}. \quad (7)$$

Figure 4 illustrates the effect of a supercurrent both in the dispersion relation of the IBS (left panel) and in the local density of states close to the interface (right panel). For $q_s = 0$, the IBS manifest in a finite LDOS for $E < \Delta$ and a sharp peak at $E = \Delta$. Qualitatively, the presence of a supercurrent breaks the symmetry with respect to inversion of the parallel momentum $\hbar q$ and leads to a splitting of the singularity at $E \simeq \Delta$ in the LDOS. Note that this implies the appearance of an induced net current on the graphene side (for $|x| \lesssim \xi$). For $E_F = 0$ the distortion of the dispersion relation for finite and small q_s is given by $E(q_s, q) = E(0, q) + (\hbar v q)^2 \eta/((\hbar v q)^2 + \Delta^2)$.

A more quantitative analysis of the effect of a supercurrent requires the estimation of the parameter E_F^S. This parameter is very much dependent on the fabrication methods and material properties of the metallic electrodes deposited on top of the graphene layer. According to the ab-initio calculations of Ref. [13] for Pd on graphene a typical estimate would be $E_F^S \sim 0.1eV$, which for a superconductor like Nb gives a ratio $E_F^S/\Delta \sim 100$. The results on Fig. 4 have been obtained for this ratio.

Conclusions: We have shown that interface bound states appear at graphene-superconductor junctions. The properties of these states are sensitive to the type of edge forming the interface, its transparency and the doping conditions of the graphene layer. We have demonstrated that the interface states evolve towards the edge states of the isolated graphene layer when the transparency of the interface is reduced. We have also shown that they can be modulated by a supercurrent flowing through the superconductor in the direction parallel to the interface. Even when our analysis has been restricted to interfaces along armchair or zig-zag edges we expect the appearance of IBSs to be a general property of any edge orientation. We also notice that inclusion of weak disorder along the interface introducing a small uncertainty in the parallel momentum δq would not prevent the emergence of IBSs provided that $\delta q \ll \Delta/\hbar v$.

As a final remark we would like to comment that the existence of IBSs induce long range superconducting correlations between distant points on the graphene layer that are close to the interface. This property could be exploited to detect crossed Andreev processes and therefore entangled electron pairs using weakly coupled STM probes on a graphene-superconductor junction, in a configuration like the one proposed in Ref. [14]. The analysis of non-local transport in this system will be the object of a separate work.

The authors would like to thank correspondence with C.W.J. Beenakker and useful discussions with J.C. Cuevas and A. Martín-Rodero. Financial support from Spanish MICINN under contracts FIS2005-06255 and FIS2008-04209, by DIB from Universidad Nacional de Colombia, and by EULA-Nanoforum is acknowledged.

[1] For a review see A. Geim and K.S. Novoselov, Nature Mat. **6**, 183 (2007).
[2] H. B. Heersche *et al.*, Nature (London) **446**, 56 (2007); A. Shailos *et al.*, Europhysics Letters **79**, 57008 (2007); F. Miao *et al.*, Science **317**, 1530 (2007); X. Du, I. Skachko and E. Andrei, Phys. Rev. B **77**, 184507 (2008).
[3] C.W.J. Beenakker, Phys. Rev. Lett. **97**, 067007 (2006).
[4] J. C. Cuevas and A. Levy Yeyati, Phys. Rev. B **74** 180501 (2006); Ali G. Moghaddam and M. Zareyan, Phys. Rev. B **74**, 241403 (2006); A. Ossipov, M. Titov and C. W. J. Beenakker, Phys. Rev. B **75**, 241401 (2007); J. Linder and A. Sudbo, Phys. Rev. Lett. **99**, 147001 (2007); J. Cayssol, Phys. Rev. Lett. **100**, 147001 (2008); D. Rainis *et al.*, Phys. Rev. B **79**, 115131 (2009); C. Benjamin and J.K. Pachos, Phys. Rev. B **79**, 155431 (2009).
[5] S. Bhattacharjee and K. Sengupta, Phys. Rev. Lett. **97**, 217001 (2006).
[6] G. Tkachov, Phys. Rev. B **76**, 235409 (2007); A.M. Black-Schaffer and S. Doniach, Phys. Rev. B **78**, 024504 (2008).
[7] P. Burset, A. Levy Yeyati and A. Martín-Rodero, Phys. Rev. B 77, 205425 (2008).
[8] M. Titov, A. Ossipov and C.W.J. Beenakker, Phys. Rev. B **75**, 045417 (2007); D.L. Bergman and K.Le Hur, arXiv:0806.0379.
[9] G.E. Blonder, M. Tinkham and T.M. Klapwijk, Phys. Rev. B **25**, 4515 (1982).
[10] K. Sengupta, R. Roy and M. Maiti, Phys. Rev. B **74**, 094505 (2006).
[11] L. Brey and H.A. Fertig, Phys. Rev. B **73**, 235411 (2006).
[12] D. Zhang, C.S. Ting and C.-R. Hu, Phys. Rev. B **70**, 172508 (2004); V. Lukic and E.J. Nicol, Phys. Rev. B **76**, 144508 (2007).
[13] N. Nemec, D. Tománek and G. Cuniberti, Phys. Rev. B **77**, 125420 (2008).
[14] J.M. Byers and M.E. Flatté, Phys. Rev. Lett. **74**, 306 (1995).